DOI 10.5012/bkcs.2010.31.04.953

Intramolecular Ion-Molecule Reactions within $Ti^+(CH_3COCH_3)_n$ Heteroclusters: Oxidation Pathway *via* C=O Bond Activation

Young-Mi Koo, Kiryong Hong,† Tae Kyu Kim,†,* and Kwang-Woo Jung*

Department of Chemistry and Institute of Nanoscience & Tech., Wonkwang University, Iksan, Chonbuk 570-749, Korea
**E-mail: kwjung@wku.ac.kr*
*†Department of Chemistry and Chemical Institute of Functional Materials, Pusan National University, Busan 609-735, Korea. *E-mail: tkkim@pusan.ac.kr*
Received November 11, 2009, Accepted March 3, 2010

A laser ablation-molecular beam/reflectron time-of-flight mass spectrometric technique was used to investigate the ion-molecule reactions that proceed within $Ti^+(CH_3COCH_3)_n$ heterocluster ions. The reactions of Ti^+ with CH_3COCH_3 clusters were found to be dominated exclusively by an oxidation reaction, which produced $TiO^+(CH_3COCH_3)_n$ clusters. These ions were attributed to the insertion of a Ti^+ ion into the C=O bond of the acetone molecule within the heteroclusters, followed by C_3H_6 elimination. The mass spectra also indicated the formation of minor sequences of heterocluster ions with the formulas $Ti^+(C_3H_4O)(CH_3COCH_3)_n$ and $TiO^+(OH)(CH_3COCH_3)_n$, which could be attributed to C-H bond insertion followed by H_2 elimination and to the sequential OH abstraction by the TiO^+ ion, respectively. Density functional theory calculations were carried out to model the structures and binding energies of both the association complexes and the relevant reaction products. The reaction pathways and energetics of the $TiO^+ + CH_2CHCH_3$ product channel are presented.

Key Words: Ion-molecule reaction, Titanium, Acetone, Heterocluster, Density functional theory

Introduction

Recent studies of the chemical reactions between transition metal ions and various organic molecules in the gas phase have yielded important insights, not only into the catalytic activity of transition metal ions, but into the reaction mechanisms and the structures of complexes that are present in many important organometallic reactions.[1-7] Among these studies, investigations of gas phase ion/solvent clusters provide a unique and experimentally accessible way to investigate the influence of solvation on the chemical reaction dynamics. Such gas phase studies have enhanced our understanding of the behavior of transition metal ions in the condensed phase.[6-7]

During the last few years, we have studied the intracluster ion-molecule reactions of Ti^+ with various organic molecules (water, alcohols, and esters) with the goal of elucidating the reactivity of Ti^+ ions and the reaction pathways that lead to heterocluster complex formation.[8-13] In particular, the reaction pathways of intracluster ion-molecule reactions of Ti^+ with ether clusters ($(CH_3OR)_n$, R = CH_3, *n*-C_3H_7, *n*-C_4H_9, *t*-C_4H_9) appeared to vary depending on the alkyl group in the ether molecule.[10] The major sequences of heterocluster ions with the formulas $Ti^+(OCH_3)_m(OR)_n$ (m = 1-3 and n = 0-2) were attributed to the insertion of Ti^+ ions into the C-O bonds of the ether molecules within the heteroclusters, followed by alkyl radical elimination. As the size of the alkyl group in the esters molecule increased, C-H and C-C bond insertions by Ti^+ ions became more favorable.[10] These results indicated that the reactivity modes of Ti^+ ions (selective bond insertions and subsequent eliminations) were unique and were not found in other transition metal ions.

The reactions of Fe^+ and Co^+ with acetone, studied by ion cyclotron resonance (ICR) and kinetic energy release distribution (KERD) experiments, mainly produced MCO^+ (M = Fe^+ or Co^+) and C_2H_6.[14,15] A reaction mechanism was proposed in which the carbonylation products form through the oxidative insertion of the metal ion into the C-C acetone bond. On the other hand, different products (MO^+ and C_3H_6) were observed from the reactions of Sc^+, Gd^+, and Pr^+ with acetone in ion beam studies.[16-18] Apart from the numerous studies of transition metal ions with acetone molecules, no detailed experimental or theoretical investigations into the mechanism and energetics of the reaction of Ti^+ ions with acetone molecules are available in the literature. Moreover only a few studies have examined the chemical reactions occurring within the heterocluster ion itself.[8-13]

In the present study, we have investigated the reaction of Ti^+ with C=O, C-C, and C-H bonds in acetone molecules within heterocluster ions. The main purpose of this work was to develop a quantitative interpretation of the reaction mechanism suggested by our observations. To probe the cluster reactivity, we examined the reaction pathways in heteroclusters using laser ablation and supersonic beam expansion techniques. In addition, density functional theory (DFT) calculations[19-22] were performed to rationalize the detailed reaction mechanism of the reaction of Ti^+ with CH_3COCH_3.

Experimental Section

Experiments. The experimental details of the ion-molecule reaction dynamics measurements have been described previously;[8-10] therefore, only a brief description is given here. Ti^+ ions were generated by focusing the third harmonic (355 nm) of a Nd:YAG laser onto a rotating titanium disk, with an illumination area of diameter ~0.5 mm. A pulse valve was employed to produce reactant clusters by supersonic expansion of the ace-

tone vapor seeded in argon with a stagnation pressure of 1 ~ 3 atm. The laser-ablated Ti^+ ions traversed the supersonic jet stream perpendicularly, where they reacted with the neutral acetone clusters. The resulting ion complexes were then skimmed by a conical skimmer (1 mm in diameter), and traveled to the extraction region of the reflectron time-of-flight mass spectrometer (RTOFMS). The cluster ions were extracted by a high-voltage pulse applied to an extraction electrode, and the ions drifted along a field-free region (1 m in length). The ions were then reflected using double-stage reflectron plates and traveled an additional 64 cm. Finally the ions were detected with a Chevron microchannel plate (MCP) detector. The mass spectra of the cluster ions were obtained using a 500 Hz digital oscilloscope. Spectral grade CH_3COCH_3 (99.5%) was used after several freeze-pump-thaw cycles to remove the dissolved atmospheric gases and other high vapor pressure impurities.

Computations. We calculated the quartet and doublet potential energy surfaces (PES) for the ion-molecule reaction of Ti^+ with CH_3COCH_3. These two states are quite close in energy and may interconvert during the reaction process.[19,20] The three-parameter hybrid B3LYP functional[23,24] was used for the DFT calculations. The molecular geometries (reactants, products, intermediates, and transition states) of both electronic states were fully optimized at B3LYP/6-311++G(d,p) levels of theory. Vibrational frequency calculations were carried out at the same level of theory to estimate all stationary points as either minima or transition states and to calculate the zero point energy (ZPE) for all reported energies. All transition states presented in this work were identified by a single imaginary frequency and were confirmed using the intrinsic reaction coordinate (IRC) method.[25,26] All DFT calculations were performed using the GAUSSIAN 03 package.[27]

Results and Discussion

Reaction pathways of Ti^+ with acetone clusters. Figure 1 shows a typical mass spectrum of ionic species produced from the reaction of Ti^+ with CH_3COCH_3 clusters seeded in 2.7 atm Ar. The spectrum was obtained using a laser pulse energy of 10 mJ/cm^2. The spectrum contained pentads of peaks corresponding to the Ti isotopes (^{46}Ti, 8.0%; ^{47}Ti, 7.3%; ^{48}Ti, 73.8%; ^{49}Ti, 5.5%; ^{50}Ti, 5.4%), with the relative intensities of these isotopomers reflecting their natural abundance. The characteristic abundance of Ti isotopomers enabled the direct identification of its complexes with acetone clusters. Unless otherwise noted, the results presented below refer to complexes involving the most abundant isotope. The prominent peaks in the mass spectrum consisted of heterocluster ions of the formula $TiO^+(CH_3COCH_3)_n$ (labeled b_n), formed through oxidation of the intact cluster ions $Ti^+(CH_3COCH_3)_n$ (labeled a_n). These oxide fragment ions were observed with up to 12 acetone units in the present experiment. This result implied that the Ti^+ ion readily reacted with CH_3COCH_3 molecules solvated within the heteroclusters. The intact cluster ions $Ti^+(CH_3COCH_3)_n$ formed from the association reaction between Ti^+ and acetone clusters, possibly followed by

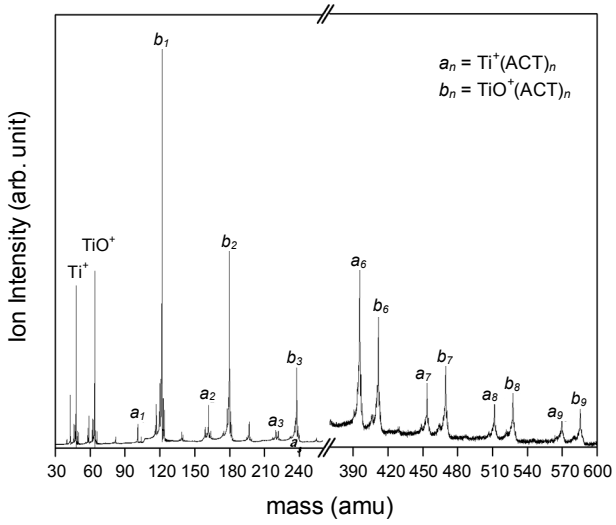

Figure 1. Mass spectrum of the cluster ions produced by reactive collisions of laser-ablated Ti^+ and acetone (CH_3COCH_3) clusters seeded in 2.7 atm Ar. The laser fluence was 10 mJ/cm^2. a_n: $Ti^+(CH_3COCH_3)_n$; b_n: $TiO^+(CH_3COCH_3)_n$. ACT denotes CH_3COCH_3.

evaporation of some acetone molecules:

$$Ti^+ + (CH_3COCH_3)_m \rightarrow [Ti^+(CH_3COCH_3)_m]^{\ddagger} \rightarrow Ti^+(CH_3COCH_3)_n + (m - n)(CH_3COCH_3) \quad (1)$$

The evaporation of several acetone molecules dissipated both the excess kinetic energy of the laser-ablated Ti^+ ions and the excess energy produced during the exothermic ion-molecule association reaction.[8,11,12]

The observation of peaks corresponding to TiO^+ indicated that the reaction was initiated by the insertion of Ti^+ into the C=O bond of an acetone molecule. We postulate that product formation proceeded through the reactions given below.

Titanium has a lower ionization energy (IE) than acetone (IE = 6.82 eV for Ti and 9.69 eV for CH_3COCH_3).[28] Hence, the positive charge on the heterocluster would be expected to reside on the Ti atom. Evidence supporting this charge distribution has been gathered in a number of beam experiments designed to study the formation of metal ion-organic molecules or metal-rare gas clusters.[29,30] The enthalpy change associated with reaction (2) was −44.4 kcal/mol, and the change associated with the formation of propene and dimethyl carbene was 13 kcal/mol.[16,18,31] Thus, the thermodynamic data indicated that $TiO^+ + H_2C{=}CHCH_3$ products would be more energetically favorable than the formation of a dimethyl carbine.

The formation of TiO^+ (*m/e* = 64) *via* reaction (2) was not surprising, considering that Ti^+ binds very strongly to oxygen atoms.[32] The initial interaction site between the Ti^+ and CH_3COCH_3 molecules within the heterocluster was envisioned to be the more basic site of the oxygen atom. The bonding in the association complex has been found to involve the formation of a dative bond requiring electron donation from the CH_3COCH_3 molecule to the 3*d* orbital of the Ti^+ ion. The Ti^+ ion then in-

$$Ti^+(CH_3COCH_3) \rightarrow [(CH_3)_2C\text{-}Ti^+\text{-}O]^{\ddagger} \rightarrow TiO^+ + H_2C{=}CHCH_3 \rightarrow TiO^+ + (CH_3)_2C: \quad (2)$$

serted into the C=O bond to form a $[C(CH_3)_2\text{-}Ti^+\text{-}O]$ intermediate, after which the $TiO^+ + H_2C{=}CHCH_3$ products formed by elimination of propene ($CH_2{=}CHCH_3$) *via* H atom migration. A similar mechanism was proposed to describe the oxidation pathway for the reaction of Ti^+ with CH_3CHO, which occurred through a C=O bond insertion process.[19,21] This mechanism was also in reasonable agreement with the results of Allison and Ridge,[16] who reported ion-molecule reactions of chlorotitanium ions $TiCl_n^+$ (n = 1-3) with CH_3COCH_3, as shown in reaction (3).

$$TiCl_n^+ + (CH_3)_2CO \rightarrow TiCl_nO^+ + C_3H_6 \ (n = 1, 2, 3) \quad (3)$$

The detailed mechanism of the oxidation pathway in the reaction of Ti^+ with CH_3COCH_3 within heteroclusters will be described in detail in the context of the calculated results in the following section.

It is interesting to note that the mass spectrum, shown in Figure 1, indicated that the chemical reactivity of Ti^+ ions within heteroclusters was strongly affected by the cluster size. The intensities of the peaks corresponding to the intact $Ti^+(CH_3COCH_3)_n$ cluster ions (a_n series) in Figure 1 were much lower than those corresponding to $TiO^+(CH_3COCH_3)_n$ (b_n series) cluster ions, and this trend was observed for all clusters with $n \leq 3$. As the cluster size increased, however, the peak intensities of the two types of cluster ions became comparable. These observations, known as product switching, demonstrate that the reactivity of the Ti^+ ions diminishes with increasing solvation by acetone molecules. This propensity has been observed in the reactions of $Mg^+ + (H_2O)_n$, described by Iwata and coworkers.[33] They found that for $n \leq 15$, the dominant species was $Mg^+(OH)(H_2O)_{n-1}$, whereas the intact ion $Mg^+(H_2O)_n$ was the major species for $n \geq 15$, and a very small quantity of $Mg^+(OH)(H_2O)_{n-1}$ was produced. The apparent quenching of the TiO^+ formation reactions (propene elimination) was attributed to the increased stabilization of $Ti^+(CH_3COCH_3)_n$ cluster ions as the degree of solvation increased. Another possible explanation for these observations is that the CH_3COCH_3 molecules surrounding the Ti^+ ions imposed an energy barrier in the oxidation pathway ($TiO^+ + H_2C{=}CHCH_3$ channel). The presence of the neutral propene within the tightly packed solvating cage of the $Ti^+(CH_3COCH_3)_n$ cluster ions was expected to increase the trapping probability with increasing cluster size.[34] Such an increase in the trapping probability would suppress the propene elimination reactions in sufficiently large clusters, producing the dominant $Ti^+(CH_3COCH_3)_n$ peaks in the high mass region of the spectrum.

To investigate the solvent effect of argon atoms on the abundance distribution of heterocluster ions, the mass spectrum was taken with an expansion of neat acetone vapor in the absence of Ar gas. A typical mass spectrum of the products of the reaction between Ti^+ and CH_3COCH_3 clusters without Ar buffer gas is shown in Figure 2. A very distinctive feature appears in this mass spectrum. In addition to the prominent $TiO^+(CH_3COCH_3)_n$ (b_n series) cluster ions, formed by C=O insertion by Ti^+ ion as discussed above, $Ti^+(C_3H_4O)(CH_3COCH_3)_n$ (labeled c_n) and $TiO^+(OH)(CH_3COCH_3)_n$ (labeled d_n) ions were also formed with low intensities. Compared to the case in which acetone vapor seeded in argon buffer gas is expanded, the acetone molecules solvating around the Ti^+ ion have a higher chance of reacting with the Ti^+ ion, resulting in a greatly enhanced peak corresponding to c_n and d_n series ions in the mass spectrum. We speculated that Ti^+ ions could insert into the C-H bonds of an CH_3COCH_3 molecule, and the subsequent H_2 elimination reactions within a single CH_3COCH_3 molecule would, therefore, produce the $Ti^+(C_3H_4O)(CH_3COCH_3)_n$ product ions (reaction (4)).

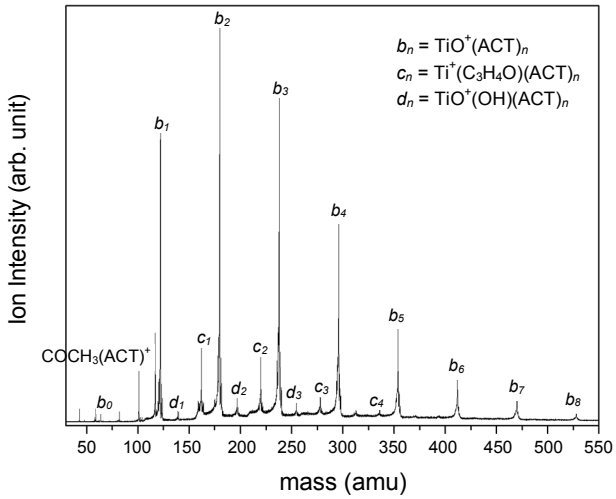

Figure 2. Mass spectrum of the cluster ions produced by reactive collisions of laser-ablated Ti^+ and neat acetone clusters without a buffer gas. The laser fluence was 15 mJ/cm^2. a_n: $Ti^+(CH_3COCH_3)_n$; b_n: $TiO^+(CH_3COCH_3)_n$; c_n: $Ti^+(C_3H_4O)(CH_3COCH_3)_n$; d_n: $TiO^+(OH)(CH_3COCH_3)_n$. ACT denotes CH_3COCH_3.

$$Ti^+(CH_3COCH_3) \rightarrow [CH_3COCH_2\text{-}Ti^+\text{-}H]^{\ddagger} \rightarrow Ti^+(C_3H_4O) + H_2 \quad (4)$$

Byrd *et al*. reported that Ti^+ reacts with small alkanes to produce 2 H or H_2 through a mechanism involving metal insertion into the C-H bond, followed by successive H eliminations from a single alkane molecule.[35] Alternatively, the formation of a TiH^+ ion from the $[CH_3COCH_2\text{-}Ti^+\text{-}H]$ intermediate *via* Ti^+-C bond rupture is unfavorable due to the relatively low dissociation energy (54.2 kcal/mol) of the Ti-H bond.[36] It might be argued that sequential H elimination reactions *via* C-H bond insertions occurred in several CH_3COCH_3 molecules within a heterocluster, which is the major reaction pathway in the reactions of Ti^+ with ethanol and dimethyl ether.[8,10] Unfortunately, the ions $(Ti^+(C_3H_4O)(CH_3COCH_3)_n)$ (H eliminations from single acetone molecule) and $(Ti^+(C_3H_5O)_2(CH_3COCH_3)_{n-1})$ (H eliminations from two acetone molecules) were difficult to distinguish because of their identical masses. However, the absence of $Ti^+(C_3H_5O)(CH_3COCH_3)_n$ product ions in the mass spectrum of Figure 2 indicated that H_2 elimination occurred in a single CH_3COCH_3 molecule only.

As a minor reaction channel, peaks corresponding to $TiO^+(OH)(CH_3COCH_3)_n$ ions (labeled d_n) also emerged, indicating up to four CH_3COCH_3 solvating units with a much lower intensity. The observation of these ions implied that TiO^+, formed from the ion-molecule reaction of $Ti^+ + CH_3COCH_3$, could

undergo a subsequent secondary reaction within a solvating CH_3COCH_3 moiety. This process proceeded *via* a sequential reaction pathway (reaction (5)).

$$[Ti^+(CH_3COCH_3)_n]^{\ddagger} \rightarrow TiO^+(CH_3COCH_3)_{n-1} + C_3H_6$$
$$\rightarrow TiO^+(OH)(CH_3COCH_3)_{n-2} + C_3H_5 + C_3H_6 \quad (5)$$

The sequential reactions of Ti^+ ions had been confirmed in our previous study of an isotope substitution reaction with CH_3OD, in which $Ti^+(OC_2H_5)_m(C_2H_5OD)_n$ (m = 1 or 2) ions were produced by consecutive insertions of Ti^+ ions into the O-D bonds of separate C_2H_5OD molecules.[8] The observation of $TiO^+(OCH_3)(CH_3OH)_n$ ions along the reaction pathway of Ti^+ ions with CH_3OH clusters also supported our finding that reaction (5) could take place in separate CH_3COCH_3 molecules. The absence of cluster ions with the formulas $TiO_2^+(OH)(CH_3COCH_3)_n$ and $TiO^+(OH)_2(CH_3COCH_3)_n$ reflected the fact that the coordination of an oxygen atom and a OH group to the Ti^+ ion reduced the ability of Ti^+ to break the C=O and C-H bonds of additional acetone molecules. Because the Ti^+ ion has three valence electrons, this decrease in reactivity was primarily attributable to the large change in binding energy that resulted from the trivalent bond formation with the O atom and the OH group.

Reaction mechanism of the oxidation pathway. As discussed, the intracluster ion-molecule reactions of Ti^+ with CH_3COCH_3 produced a major sequence of $TiO^+(CH_3COCH_3)_n$ ions, which was attributed to the insertion of Ti^+ into the C=O bond of CH_3COCH_3, followed by C_3H_6 elimination. To interpret the experimental findings and gain further insight into the reaction mechanism, we performed electronic structure calculations to propose possible oxidation pathways for the reaction between Ti^+ and CH_3COCH_3. Because the chemical reactivity of transition metal ions with organic molecules is greatly influenced by the spin state of the metal ion, we considered the quartet and doublet states of the Ti^+ ion in our model for the ion-molecule reaction of Ti^+ with CH_3COCH_3.

The geometries of the stationary points in both quartet and doublet electronic states are depicted in Figure 3, where the superscript denotes the spin multiplicity. Figure 4 shows the potential energy surface diagram associated with the oxidation process, where the energies of the reactants, products, intermediate states, and transition states were obtained at the B3LYP/6-311++G(d,p) level. The oxidation reaction took place by processes that included: (i) C=O bond activation of CH_3COCH_3 *via* initial complexation with Ti^+ ions, (ii) insertion of Ti^+ into the C=O bond, and (iii) intramolecular H atom migration. First, the excited state of Ti^+ (^{2}F) was computed to lie 13.02 kcal/mol above the ground state of Ti^+ (^{4}F) at the B3LYP/6-311++G(d,p) level, which was in excellent agreement with the experimental value of 13.03 kcal/mol.[37] Moreover, the calculated bond dissociation energy (153.8 kcal/mol) of the TiO^+ ($^2\Delta$) ion was also consistent with the experimental (159.8 kcal/mol)[38] and theoretical (155.1 kcal/mol) values,[39] which demonstrated the accuracy of our calculated results.

As shown in Figure 4, the reaction began with the approach of a Ti^+ ion to CH_3COCH_3, leading to the association complexes ^{4}**1** and ^{2}**1**. These complexes were calculated to be more stable, by 64.42 kcal/mol (^{4}**1**) and 50.93 kcal/mol (^{2}**1**), respectively,

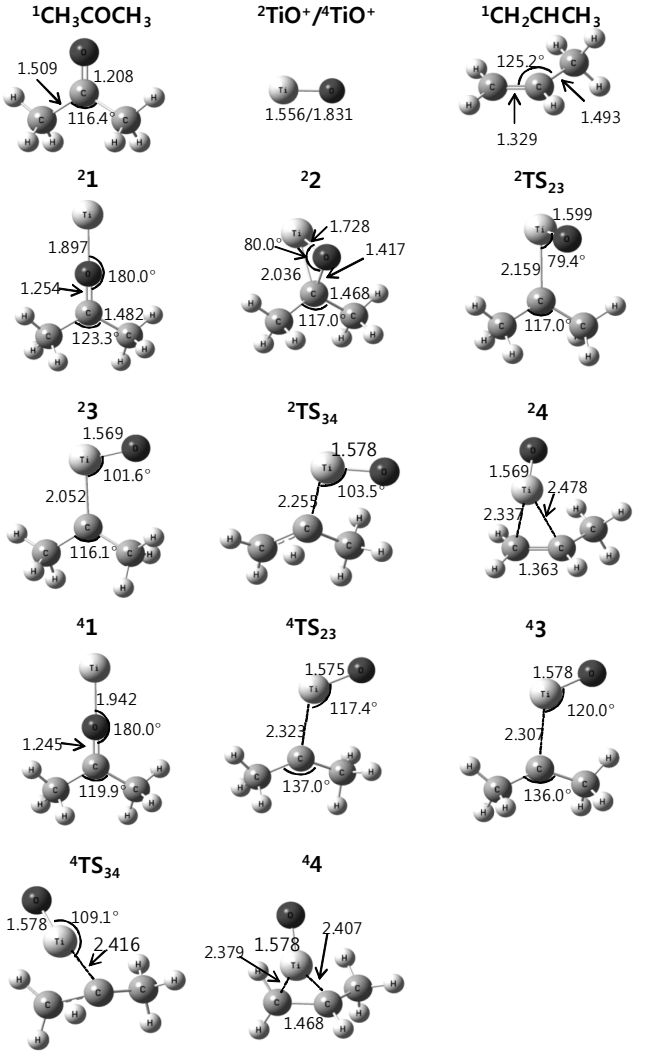

Figure 3. Selected geometrical parameters (bond lengths in Å and angles in degrees) of the optimized structures for the stationary points in the doublet and quartet potential energy surfaces for the oxidation process of CH_3COCH_3 by Ti^+.

than the isolated reactants. Figure 3 shows that both association structures were characterized by linear binding ($\angle Ti^+$-O-C = 180°), remarkably different from the bent geometry of the Ni^+-CH_3COCH_3 complex ($\angle Ni^+$-O-C = 138.8°), which produces $Ni^+CO + C_2H_6$ fragments.[22] Considering the equilibrium distance of Ti^+-O bonds in ^{4}**1** (1.942 Å) and ^{2}**1** (1.897 Å) in Figure 3, the interaction between Ti^+ and CH_3COCH_3 was considered to be electrostatic in nature. Once the association complexes (^{4}**1** and ^{2}**1**) formed, the oxidation process was initiated by the Ti^+ insertion into the C=O bond *via* the formation of a stable three-membered complex ^{2}**2**. Compared to the association complexes ^{4}**1** and ^{2}**1**, the geometrical changes of the intermediate ^{2}**2** were characterized by the lengthening of the C-O bond and the slight contraction of the C-C bonds. This was most likely due to the polarization of the oxygen charges toward Ti^+, which weakened the C-O bond.[19,21] It is quite surprising that our current calculations produced only the ^{2}**2** intermediate without a transition state for either the double or quartet states. Therefore,

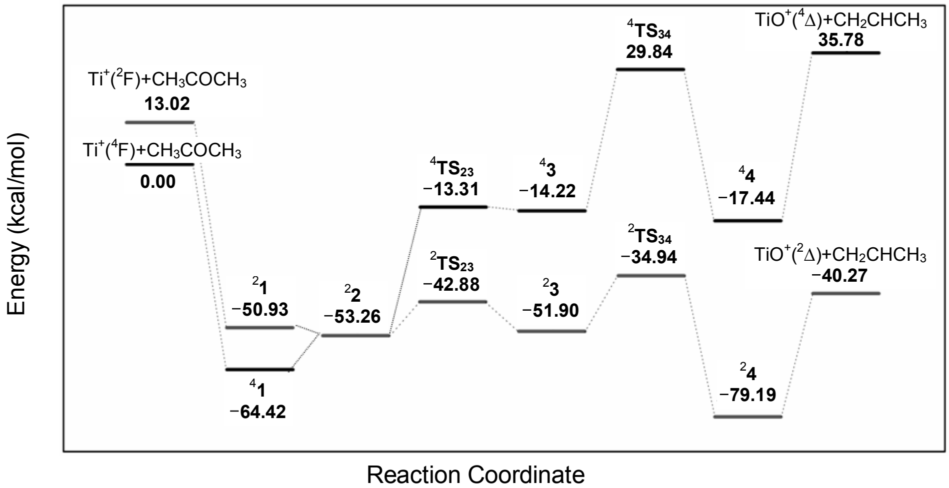

Figure 4. Potential energy surfaces of the Ti^+ insertion into the C=O bond at the B3LYP/6-311++G(d,p) level. The related optimized structures are depicted in Figure 3.

it could be assumed that intersystem crossing took place between the ground spin state (^{4}F) and the doublet spin state (^{2}F) reaction pathways (^{4}**1** → ^{2}**2**). Similarly, intersystem crossing between the doublet and quartet spin states has been observed in gas phase ion-molecule reactions of Ti^+ with NH_3, CH_4,[40] CH_3OCH_3,[19] and CH_3CHO.[21] While we cannot exclude all the possible reactions of electronically excited Ti^+ (^{2}F) ions, we believe that the observed reaction patterns in the current experiments are mainly due to ground-state reactions. This is because the laser-ablated Ti^+ ions are likely to be efficiently quenched by their collision with the supersonic beam of CH_3COCH_3/Ar.

As can be seen in Figure 3, a scissor vibration of O-Ti^+-C can convert the intermediate **2** into the complex **3** through $^2TS_{23}$ or $^4TS_{23}$. Compared to the ^{2}**2** intermediate, the C-O bond distance was substantially elongated due to the weak C-O bond strength in both $^2TS_{23}$ and $^4TS_{23}$; thus the Ti^+ ion could readily insert into the C=O bond. In the ^{2}**3** and ^{4}**3** intermediates, the Ti^+-O bond was positioned in the plane defined by the Ti^+-C and C-C bonds. Intramolecular H atom migration from the CH_3 group to the central carbon atom of the ^{2}**3** and ^{4}**3** intermediates yielded the ^{2}**4** and ^{4}**4** intermediates, respectively, *via* transition states $^2TS_{34}$ and $^4TS_{34}$. The energy of the transition state $^2TS_{34}$ was −34.94 kcal/mol more stable than the energies of the separate reactants, and represented the largest barrier along the doublet surface of the C=O bond insertion pathway. This fact strongly suggests that the hydrogen migration process between the two carbon atoms is the rate-determining step of the oxidation process. The most stable energy of the ^{2}**4** intermediate (−79.19 kcal/mol) along the oxidation pathway presumably arose from the strong stabilization of both the $TiO^+(^2\Delta)$ ion and H_2CHCH_3.[21]

The geometrical parameters of ^{2}**4** were very close to those of $TiO^+(^2\Delta)$ and CH_2CHCH_3-free molecules, except that the intermediate ^{2}**4** had a slightly longer C=C bond (1.363 Å) compared to that of the free CH_2CHCH_3 molecule (1.329 Å). This observation indicates that the 3*d* orbital of Ti^+ interacts with the π* orbital of the C=C bond. We also considered the possibility of C_3H_6 (cyclopropane) formation as a final product, but cyclopropane lay 5.2 kcal/mol higher in energy than CH_2CHCH_3 (propene). The overall reaction energies, *via* C=O bond insertion by Ti^+, were calculated to be 35.78 kcal/mol (endothermic) for the $TiO^+(^4\Delta)$ + CH_2CHCH_3 channel and 40.27 kcal/mol (exothermic) for the $TiO^+(^2\Delta)$ + CH_2CHCH_3 channel, in good agreement with the experimental values.[16,18,31] Therefore, our results indicate that the oxidation of CH_3COCH_3 by Ti^+ occurs through five elementary steps: association complexation, intersystem crossing, Ti^+ insertion into the C=O bond, hydrogen migration, and fragmentation.

Conclusions

In the present study, we investigated intracluster ion-molecule reactions within mixed $Ti^+(CH_3COCH_3)_n$ heterocluster ions using a combination of laser ablation and supersonic beam expansion. The primary reactions produced a major sequence of $TiO^+(CH_3COCH_3)_n$ ions, which was attributed to the insertion of Ti^+ ions into the C=O bond of the CH_3COCH_3 molecule, followed by H atom migration and CH_2CHCH_3 fragmentation. The observation of $Ti^+(C_3H_4O)(CH_3COCH_3)_n$ ions was interpreted as a minor reaction channel consisting of C-H bond insertion followed by successive H_2 elimination from the CH_3COCH_3 molecule. In addition, $TiO^+(OH)(CH_3COCH_3)_n$ ions were ascribed to the sequential OH abstraction by TiO^+ ions formed from the primary reaction within the heteroclusters. DFT calculations were performed to develop a detailed mechanistic model for the oxidation process in the ion-molecule reaction of Ti^+ + CH_3COCH_3. The results indicate that the oxidation process of CH_3COCH_3 by Ti^+ proceeds through five elementary steps − association complexation, intersystem crossing, Ti^+ insertion into the C=O bond, H atom migration, and fragmentation − in which the H transfer process was predicted to be the rate-determining step.

Acknowledgments. This work was supported by a Korea Research Foundation Grant funded by the Korean Government (MOEHRD) (R05-2004-000-10132-0), by Grant No. R-01-

2008-000-20717-0 from the Basic Research Program of the Korea Science and Engineering Foundation, Republic of Korea, and by Pusan National University Research Grant, 2007. One of the authors (K.-W. Jung) also gratefully acknowledges the financial support of Energy & Resource Technology Development Program (2009T100100674) under the Ministry of Knowledge Economy and also by the Korea Institute of Marine & Technology Promotion in 2009.

References

1. Böhme, D. K.; Schwartz, H. *Angew. Chem. Int. Ed.* **2005**, *44*, 2336.
2. *Advances in Metal and Semiconductor Clusters*; Duncan M. A., Ed.; Elsevier: Amsterdam, 2001; Vol. 5.
3. Liu, H.; Hu, Y.; Yang, S.; Guo, W.; Fu, Q.; Wang, L. *J. Phys. Chem. A* **2006**, *110*, 4389.
4. Velasquez, J.; Pillai, E. D.; Carnegie, P. D.; Duncan, M. A. *J. Phys. Chem. A* **2006**, *110*, 2325.
5. Zheng, G.; Kemper, P. R.; Bowers, M. *Int. J. Mass Spectrom.* **2001**, *265*, 210.
6. Lee, M. A.; Nam, S. H.; Park, H. S.; Cheong, N. R.; Ryu, S.; Song, J. K.; Park, S. M. *Bull. Korean Chem. Soc.* **2008**, *29*, 2109.
7. Choi, S.-S.; Ha, S.-H. *Bull. Korean Chem. Soc.* **2007**, *28*, 2508.
8. Koo, Y. M.; Kim, J. H.; Lee, H.; Jung, K. W. *J. Phys. Chem. A* **2002**, *106*, 2465.
9. Koo, Y. M.; An, J. H.; Yoo, S. K.; Jung, K. W. *Int. J. Mass Spectrom.* **2003**, *226*, 305.
10. Koo, Y. M.; Kim, M. K.; Jung, K. W. *Int. J. Mass Spectrom.* **2005**, *243*, 97.
11. Koo, Y. M.; Kim, T. K.; Jung, D. W.; Jung, K. W. *J. Phys. Chem. A* **2006**, *110*, 13724.
12. Kim, T. K.; Koo, Y. M.; Jung, D. W.; Jung, K. W. *Bull. Korean Chem. Soc.* **2008**, *29*, 4.
13. Kim, T. K.; Koo, Y. M.; Jung, D. W.; Jung, K. W. *Bull. Korean Chem. Soc.* **2008**, *29*, 2183.
14. Burnier, R. C.; Byrd, G. D.; Freiser, B. S. *Anal. Chem.* **1980**, *52*, 1641.
15. Hanratty, M. A.; Beauchamp, J. L.; Illies, A. J.; van Koppen, P.; Bowers, M. T. *J. Am. Chem. Soc.* **1988**, *110*, 1.
16. Allison, J.; Ridge, D. P. *J. Am. Chem. Soc.* **1978**, *100*, 163.
17. Tolbert, M. A.; Beauchamp, J. L. *J. Am. Chem. Soc.* **1984**, *106*, 8117.
18. Schilling, J. B.; Beauchamp, J. L. *J. Am. Chem. Soc.* **1988**, *110*, 15.
19. Zhao, L. M.; Zhang, R. R.; Guo, W. Y.; Lu, X. Q. *Chem. Phys. Lett.* **2006**, *431*, 56.
20. Ding, N.; Zhang, S. G.; Chen, X. X. *Chem. Phys. Lett.* **2008**, *458*, 33.
21. Wang, Y. C.; Liu, Z. Y.; Geng, Z. Y.; Yang, X. Y. *Chem. Phys. Lett.* **2006**, *427*, 271.
22. Chen, X. F.; Guo, W. Y.; Zhao, L. M.; Fu, Q. T. *Chem. Phys. Lett.* **2006**, *432*, 27.
23. Becke, D. A. *J. Chem. Phys.* **1993**, *98*, 1372.
24. Lee, C.; Yang, W.; Parr, R. G. *Phys. Rev. B* **1990**, *94*, 5523.
25. Gonzalez, C.; Schlegel, H. B. *J. Chem. Phys.* **1989**, *90*, 2154.
26. Gonzalez, C.; Schlegel, H. B. *J. Phys. Chem.* **1990**, *94*, 5523.
27. Gaussian 03, R. E., Frisch, M. J.; Trucks, G. W.; Schlegel, H. B.; Scuseria, G. E.; Robb, M. A.; Cheeseman, J. R.; Montgomery, Jr., J. A.; Vreven, T.; Kudin, K. N.; Burant, J. C.; Millam, J. M.; Iyengar, S. S.; Tomasi, J.; Barone, V.; Mennucci, B.; Cossi, M.; Scalmani, G.; Rega, N.; Petersson, G. A.; Nakatsuji, H.; Hada, M.; Ehara, M.; Toyota, K.; Fukuda, R.; Hasegawa, J.; Ishida, M.; Nakajima, T.; Honda, Y.; Kitao, O.; Nakai, H.; Klene, M.; Li, X.; Knox, J. E.; Hratchian, H. P.; Cross, J. B.; Bakken, V.; Adamo, C.; Jaramillo, J.; Gomperts, R.; Stratmann, R. E.; Yazyev, O.; Austin, A. J.; Cammi, R.; Pomelli, C.; Ochterski, J. W.; Ayala, P. Y.; Morokuma, K.; Voth, G. A.; Salvador, P.; Dannenberg, J. J.; Zakrzewski, V. G.; Dapprich, S.; Daniels, A. D.; Strain, M. C.; Farkas, O.; Malick, D. K.; Rabuck, A. D.; Raghavachari, K.; Foresman, J. B.; Ortiz, J. V.; Cui, Q.; Baboul, A. G.; Clifford, S.; Cioslowski, J.; Stefanov, B. B.; Liu, G.; Liashenko, A.; Piskorz, P.; Komaromi, I.; Martin, R. L.; Fox, D. J.; Keith, T.; Al-Laham, M. A.; Peng, C. Y.; Nanayakkara, A.; Challacombe, M.; Gill, P. M. W.; Johnson, B.; Chen, W.; Wong, M. W.; Gonzalez, C.; and Pople, J. A.; Gaussian, Inc., Wallingford CT, 2004.
28. Koppel, I. A.; Molder, U. H.; Pikver, R. J. *Org. React. Tartu.* **1983**, *20*, 45.
29. Pilgram, J. S.; Yeh, C. S.; Berry, K. R.; Duncan, M. A. *J. Chem. Phys.* **1994**, *100*, 7945.
30. Weis, P.; Kemper, P. R.; Bower, M. T. *J. Phys. Chem. A* **1997**, *101*, 8207.
31. Chase, P. M. W.; Curnutt, J. L.; Prophet, H.; McDonald, R. A.; Syverud, A. N. *J. Phys. Chem. Ref. Data* **1975**, *4*, 1.
32. Clemmer, D. E.; Elking, J. L.; Aristov, N.; Armentrout, P. B. *J. Chem. Phys.* **1991**, *95*, 3387.
33. Misaizu, F.; Sanekata, M.; Fuke, K.; Iwata, S. *J. Chem. Phys.* **1994**, *100*, 1161.
34. Lu, W.; Yang, S. *J. Phys. Chem. A* **1998**, *102*, 825.
35. Byrd, G. D.; Burnier, R. C.; Freiser, B. S. *J. Am. Chem. Soc.* **1982**, *104*, 3565.
36. Sunderlin, L. S.; Armentrout, P. B. *J. Phys. Chem.* **1988**, *92*, 1209.
37. Moore, C. E. *ATOMIC ENERGY LEVELS*; NSRD-NBS, USA, US Government Printing Office: Washington, D. C., 1971; Vol. 1.
38. Schröder, D.; Schwarz, H. *Angew. Chem. Int. Ed.* **1995**, *34*, 1973.
39. Shiota, Y.; Yoshizawa, K. *J. Am. Chem. Soc.* **2000**, *122*, 12317.
40. Sicilia, E.; Russo, N. *J. Am. Chem. Soc.* **2002**, *124*, 1471.